

**Electrically tunable Gilbert damping in van der Waals heterostructures of two-dimensional ferromagnetic metals and ferroelectrics**Liang Qiu,<sup>1</sup> Zequan Wang,<sup>1</sup> Xiao-Sheng Ni,<sup>1</sup> Dao-Xin Yao<sup>1,2</sup> and Yusheng Hou<sup>1,\*</sup>**AFFILIATIONS**<sup>1</sup> Guangdong Provincial Key Laboratory of Magnetoelectric Physics and Devices, State Key Laboratory of Optoelectronic Materials and Technologies, Center for Neutron Science and Technology, School of Physics, Sun Yat-Sen University, Guangzhou, 510275, China<sup>2</sup> International Quantum Academy, Shenzhen 518048, China**ABSTRACT**

Tuning the Gilbert damping of ferromagnetic (FM) metals via a nonvolatile way is of importance to exploit and design next-generation novel spintronic devices. Through systematical first-principles calculations, we study the magnetic properties of the van der Waals heterostructure of two-dimensional FM metal CrTe<sub>2</sub> and ferroelectric (FE) In<sub>2</sub>Te<sub>3</sub> monolayers. The ferromagnetism of CrTe<sub>2</sub> is maintained in CrTe<sub>2</sub>/In<sub>2</sub>Te<sub>3</sub> and its magnetic easy axis can be switched from in-plane to out-of-plane by reversing the FE polarization of In<sub>2</sub>Te<sub>3</sub>. Excitingly, we find that the Gilbert damping of CrTe<sub>2</sub> is tunable when the FE polarization of In<sub>2</sub>Te<sub>3</sub> is reversed from upward to downward. By analyzing the *k*-dependent contributions to the Gilbert damping, we unravel that such tunability results from the changed intersections between the bands of CrTe<sub>2</sub> and Fermi level on the reversal of the FE polarizations of In<sub>2</sub>Te<sub>3</sub> in CrTe<sub>2</sub>/In<sub>2</sub>Te<sub>3</sub>. Our work provides an appealing way to electrically tailor Gilbert dampings of two-dimensional FM metals by contacting them with ferroelectrics.

\*Authors to whom correspondence should be addressed:

[Yusheng Hou, houysh@mail.sysu.edu.cn]

This is the author's peer reviewed, accepted manuscript. However, the online version of record will be different from this version once it has been copyedited and typeset.

PLEASE CITE THIS ARTICLE AS DOI: 10.1063/5.0145401

Since the atomically thin long-range ferromagnetic (FM) orders at finite temperatures are discovered in  $\text{CrI}_3^1$  monolayer (ML) and  $\text{Cr}_2\text{Ge}_2\text{Te}_6^2$  bilayer, two-dimensional (2D) van der Waals (vdW) FM materials have attracted intensive attention.<sup>3-5</sup> Up to now, many novel vdW ferromagnets such as  $\text{Fe}_3\text{GeTe}_2$ ,<sup>6</sup>  $\text{Fe}_5\text{GeTe}_2$ ,<sup>7</sup>  $\text{VSe}_2$ ,<sup>8,9</sup> and  $\text{MnSe}_2$ <sup>10</sup> have been synthesized in experiments. Due to the intrinsic ferromagnetism in these vdW FM materials, it is highly fertile to engineer emergent phenomena through magnetic proximity effect in their heterostructures.<sup>11</sup> For instance, an unprecedented control of the spin and valley pseudospins in  $\text{WSe}_2$  ML is reported in  $\text{CrI}_3/\text{WSe}_2$ .<sup>12</sup> By contacting the thin films of three-dimensional topological insulators and graphene with  $\text{CrI}_3$ , high-temperature quantum anomalous Hall effect and vdW spin valves are proposed in  $\text{CrI}_3/\text{Bi}_2\text{Se}_3/\text{CrI}_3$ <sup>13</sup> and  $\text{CrI}_3/\text{graphene}/\text{CrI}_3$ ,<sup>14</sup> respectively. On the other hand, the magnetic properties of these vdW FM materials can also be controlled by means of external perturbations such as gating and moiré patterns.<sup>3</sup> In  $\text{CrI}_3$  bilayer, Huang *et al.* observed a voltage-controlled switching between antiferromagnetic (AFM) and FM states.<sup>15</sup> Via an ionic gate, Deng *et al.* even increased the Curie temperature ( $T_C$ ) of the thin flake of vdW FM metal  $\text{Fe}_3\text{GeTe}_2$  to room temperature, which is much higher than its bulk  $T_C$ .<sup>6</sup> Very recently, Xu *et al.* demonstrated a coexisting FM and AFM state in a twisted bilayer  $\text{CrI}_3$ .<sup>16</sup> These indicate that vdW FM materials are promising platforms to design and implement spintronic devices in the 2D limit.<sup>4,11</sup>

Recently, of great interest is the emergent vdW magnetic material  $\text{CrTe}_2$  which is a new platform for realizing room-temperature intrinsic ferromagnetism.<sup>17,18</sup> Especially,  $\text{CrTe}_2$  exhibits greatly tunable magnetism. In the beginning, its ground state is believed to be the nonmagnetic  $2H$  phase,<sup>19</sup> while several later researches suggest that either the FM or AFM  $1T$  phases should be the ground state of  $\text{CrTe}_2$ .<sup>17,18,20-23</sup> Currently, the consensus is that the structural ground state of  $\text{CrTe}_2$  is the  $1T$  phase. With respect to its magnetic ground state, a first-principles study shows that the FM and AFM ground states in  $\text{CrTe}_2$  ML depend on its in-plane lattice constants.<sup>24</sup> It is worth noting that the  $T_C$  of FM  $\text{CrTe}_2$  down to the few-layer limit can be higher than 300 K,<sup>18</sup> making it have wide practical application prospects in spintronics.

This is the author's peer reviewed, accepted manuscript. However, the online version of record will be different from this version once it has been copyedited and typeset.

PLEASE CITE THIS ARTICLE AS DOI: 10.1063/5.0145401

Building heterostructures of FM and ferroelectric (FE) materials offers an effective way to control nonvolatile magnetism via an electric field. Experimentally, Eerenstein *et al.* presented an electric-field-controlled nonvolatile converse magnetoelectric effect in a multiferroic heterostructure  $\text{La}_{0.67}\text{Sr}_{0.33}\text{MnO}_3/\text{BaTiO}_3$ .<sup>25</sup> Later, Zhang *et al.* reported an electric-field-driven control of nonvolatile magnetization in a heterostructure of FM amorphous alloy  $\text{Co}_{40}\text{Fe}_{40}\text{B}_{20}$  and FE  $\text{Pb}(\text{Mg}_{1/3}\text{Nb}_{2/3})_{0.7}\text{Ti}_{0.3}\text{O}_3$ .<sup>26</sup> Theoretically, Chen *et al.* demonstrated based on first-principles calculations that the interlayer magnetism of  $\text{CrI}_3$  bilayer in  $\text{CrI}_3/\text{In}_2\text{Se}_3$  is switchable between FM and AFM couplings by the nonvolatile control of the FE polarization direction of  $\text{In}_2\text{Se}_3$ .<sup>27</sup> In spite of these interesting findings, using FE substrates to electrically tune the Gilbert damping of ferromagnets, an important factor determining the operation speed of spintronic devices, is rarely investigated in 2D FM/FE vdW heterostructures. Therefore, it is of great importance to explore the possibility of tuning the Gilbert damping in such kind of heterostructures.

In this work, we first demonstrate that the magnetic ground state of 1T-phase  $\text{CrTe}_2$  ML will change from the zigzag AFM (denoted as z-AFM) to FM orders with increasing its in-plane lattice constants. By building a vdW heterostructure of  $\text{CrTe}_2$  and FE  $\text{In}_2\text{Te}_3$  MLs, we show that the magnetic easy axis of  $\text{CrTe}_2$  can be tuned from in-plane to out-of-plane by reversing the FE polarization of  $\text{In}_2\text{Te}_3$ , although its ferromagnetism is kept. Importantly, we find that the Gilbert damping of  $\text{CrTe}_2$  is tunable with a wide range on reversing the FE polarization of  $\text{In}_2\text{Te}_3$  from upward to downward. Through looking into the  $k$ -dependent contributions to the Gilbert damping, we reveal that such tunability originates from the changed intersections between the bands of  $\text{CrTe}_2$  and Fermi level when the FE polarizations of  $\text{In}_2\text{Te}_3$  is reversed in  $\text{CrTe}_2/\text{In}_2\text{Te}_3$ . Our work demonstrates that putting 2D vdW FM metals on FE substrates is an attractive method to electrically tune their Gilbert dampings.

$\text{CrTe}_2$ , a member of the 2D transition metal dichalcogenide family, can potentially crystallize into several different layered structures such as 1T, 1T<sub>d</sub>, 1H and 2H phases.<sup>28</sup> It is believed that the 1T phase is the most stable among all of these possible phases in

This is the author's peer reviewed, accepted manuscript. However, the online version of record will be different from this version once it has been copyedited and typeset.

PLEASE CITE THIS ARTICLE AS DOI: 10.1063/5.0145401

both bulk and ML. This phase has a hexagonal lattice and belongs to the  $P3m1$  space group, with each Cr atom surrounded by the octahedrons of Te atoms (Fig. 1a). In view of the hot debates on the magnetic ground state in CrTe<sub>2</sub> ML, we establish a  $2 \times 2\sqrt{3}$  supercell and calculate the total energies of several different magnetic structures (Fig. S1 in Supplementary Materials) when its lattice constant varies from 3.65 to 4.00 Å. As shown in Fig. 1b, our calculations show that z-AFM order is the magnetic ground state when the lattice constant is from 3.65 to 3.80 Å. By contrast, the FM order is the magnetic ground state when the lattice constant is in the range from 3.80 to 4.00 Å. Note that our results are consistent with the experimentally observed z-AFM<sup>23</sup> and FM<sup>29</sup> orders in CrTe<sub>2</sub> with a lattice constant of 3.70 and 3.95 Å, respectively. Since we are interested in the Gilbert damping of ferromagnets and the experimentally grown CrTe<sub>2</sub> on ZrTe<sub>2</sub> has a lattice constant of 3.95 Å,<sup>29</sup> we will focus on CrTe<sub>2</sub> ML with this lattice constant hereinafter.

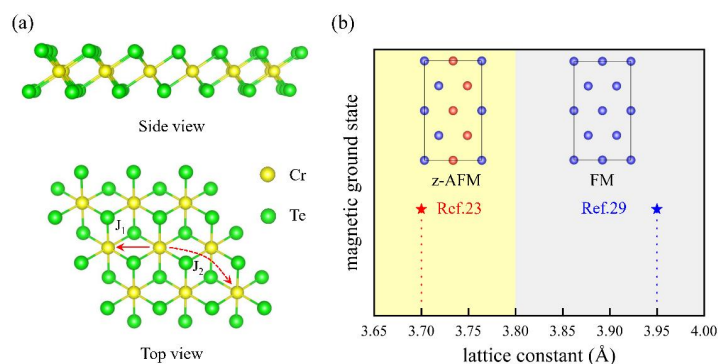


FIG. 1. (a) Side (the top panel) and top (the bottom panel) views of CrTe<sub>2</sub> ML. The NN and second-NN exchange paths are shown by red arrows in the top view. (b) The phase diagram of the magnetic ground state of CrTe<sub>2</sub> ML with different lattice constants. Insets show the schematic illustrations of the z-AFM and FM orders. The up and down spins are indicated by the blue and red balls, respectively. The stars highlight the experimental lattice constants of CrTe<sub>2</sub> in Ref.23 and Ref.29.

To obtain an deeper understanding on the ferromagnetism of CrTe<sub>2</sub> ML, we adopt a spin Hamiltonian consisting of Heisenberg exchange couplings and single-ion magnetic anisotropy (SIA) as follows:<sup>30</sup>

$$H = J_1 \sum_{\langle ij \rangle} S_i \cdot S_j + J_2 \sum_{\langle\langle ij \rangle\rangle} S_i \cdot S_j - A \sum_i (S_i^z)^2 \quad (1)$$

In Eq. (1),  $J_1$  and  $J_2$  are the nearest neighbor (NN) and second-NN Heisenberg exchange couplings. Note that a negative (positive)  $J$  means a FM (AFM) Heisenberg exchange couples. Besides,  $A$  parameterizes the SIA term. First of all, our DFT calculations show that the magnetic moment of CrTe<sub>2</sub> ML is 3.35  $\mu_B$ /Cr, consistent with previous DFT calculations.<sup>31</sup> As shown in Table I, the calculated  $J_1$  and  $J_2$  are both FM and  $J_1$  is much stronger than  $J_2$ . Both FM  $J_1$  and  $J_2$  undoubtedly indicate that CrTe<sub>2</sub> ML has a FM magnetic ground state. Finally, the SIA parameter  $A$  is obtained by calculating the energy difference between two FM states with out-of-plane and in-plane magnetizations. Our calculations obtain  $A=1.81$  meV/Cr, indicating that CrTe<sub>2</sub> ML has an out-of-plane magnetic easy axis. Hence, our calculations show that CrTe<sub>2</sub> ML exhibits an out-of-plane FM order, consistent with experimental observations.<sup>29</sup>

TABLE I. Listed are the in-plane lattice constants  $a$ , Heisenberg exchange couplings  $J$  (in unit of meV) and SIA (in unit of meV/Cr) of CrTe<sub>2</sub> ML and CrTe<sub>2</sub>/In<sub>2</sub>Te<sub>3</sub>.

| System   | $a$ (Å) | $J_1$  | $J_2$ | $A$   |
|--|---------|--------|-------|-------|
| CrTe <sub>2</sub>                                      | 3.95    | -24.56 | -0.88 | 1.81  |
| CrTe <sub>2</sub> /In <sub>2</sub> Te <sub>3</sub> (↑) | 7.90    | -20.90 | -1.80 | -1.44 |
| CrTe <sub>2</sub> /In <sub>2</sub> Te <sub>3</sub> (↓) | 7.90    | -19.33 | -0.88 | 0.16  |

To achieve an electrically tunable Gilbert damping in CrTe<sub>2</sub> ML, we establish its vdW heterostructure with FE In<sub>2</sub>Te<sub>3</sub> ML. In building this heterostructure, we stack a 2×2 supercell of CrTe<sub>2</sub> and a  $\sqrt{3} \times \sqrt{3}$  supercell of In<sub>2</sub>Te<sub>3</sub> along the (001) direction. Because the magnetic properties of CrTe<sub>2</sub> ML are the primary topic and the electronic properties of In<sub>2</sub>Te<sub>3</sub> ML are basically not affected by a strain (Fig. S2), we stretch the lattice constant of the latter to match that of the former. Fig. 2a shows the most stable

This is the author's peer reviewed, accepted manuscript. However, the online version of record will be different from this version once it has been copyedited and typeset.

PLEASE CITE THIS ARTICLE AS DOI: 10.1063/5.0145401

stacking configuration in  $\text{CrTe}_2/\text{In}_2\text{Te}_3$  with an upward FE polarization [denoted as  $\text{CrTe}_2/\text{In}_2\text{Te}_3(\uparrow)$ ]. At the interface in this configuration, one of four Cr atoms and one of four Te atoms at the bottom of  $\text{CrTe}_2$  sits on the top of the top-layer Te atoms of  $\text{In}_2\text{Te}_3$ . In  $\text{CrTe}_2/\text{In}_2\text{Te}_3$  with a downward FE polarization [denoted as  $\text{CrTe}_2/\text{In}_2\text{Te}_3(\downarrow)$ ], the stacking configuration at its interface is same as that in  $\text{CrTe}_2/\text{In}_2\text{Te}_3(\uparrow)$ . The only difference between  $\text{CrTe}_2/\text{In}_2\text{Te}_3(\uparrow)$  and  $\text{CrTe}_2/\text{In}_2\text{Te}_3(\downarrow)$  is that the middle-layer Te atoms of  $\text{In}_2\text{Te}_3$  in the former is farther to  $\text{CrTe}_2$  than that in the latter (Fig. 2a and 2c). It is noteworthy that the bottom-layer Te atoms of  $\text{CrTe}_2$  do not stay at a plane anymore in the relaxed  $\text{CrTe}_2/\text{In}_2\text{Te}_3$  (see more details in Fig. S3), suggesting non-negligible interactions between  $\text{CrTe}_2$  and  $\text{In}_2\text{Te}_3$ .

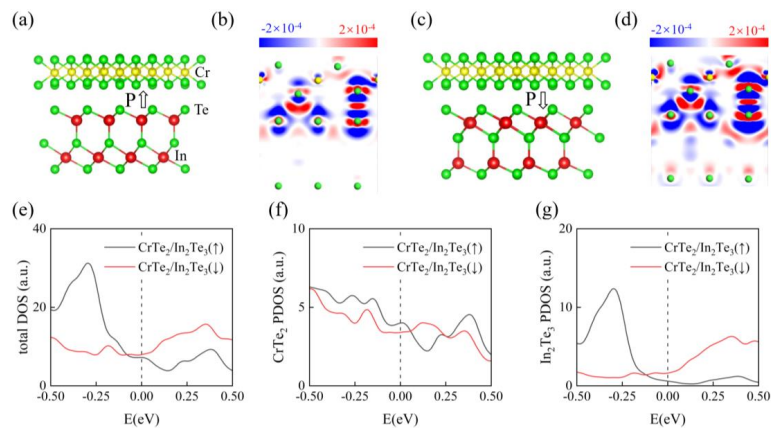


FIG. 2. (a) The schematic stacking configuration and (b) charge density difference  $\Delta\rho$  of  $\text{CrTe}_2/\text{In}_2\text{Te}_3(\uparrow)$ . (c) and (d) same as (a) and (b) but for  $\text{CrTe}_2/\text{In}_2\text{Te}_3(\downarrow)$ . In (b) and (d), color bar indicates the weight of negative (blue) and positive (red) charge density differences. (e) The total DOS of  $\text{CrTe}_2/\text{In}_2\text{Te}_3$ . (f) and (g) show the PDOS of  $\text{CrTe}_2$  and  $\text{In}_2\text{Te}_3$  in  $\text{CrTe}_2/\text{In}_2\text{Te}_3$ , respectively. In (e)-(g), upward and downward polarizations are indicated by black and red lines, respectively.

To shed light on the effect of the FE polarization of  $\text{In}_2\text{Te}_3$  on the electronic property of  $\text{CrTe}_2/\text{In}_2\text{Te}_3$ , we first investigate the spatial distribution of charge density

difference  $\Delta\rho = \rho_{\text{CrTe}_2/\text{In}_2\text{Te}_3} - \rho_{\text{CrTe}_2} - \rho_{\text{In}_2\text{Te}_3}$  with different FE polarization directions. As shown in Fig. 2b and 2d, we see that there is an obvious charge transfer at the interfaces of both  $\text{CrTe}_2/\text{In}_2\text{Te}_3(\uparrow)$  and  $\text{CrTe}_2/\text{In}_2\text{Te}_3(\downarrow)$ , which is further confirmed by the planar averaged  $\Delta\rho$  (Fig. S4). Additionally, the charge transfer in  $\text{CrTe}_2/\text{In}_2\text{Te}_3(\uparrow)$  is distinctly less than that in  $\text{CrTe}_2/\text{In}_2\text{Te}_3(\downarrow)$ . Fig. 2e shows that the total density of states (DOS) near Fermi level are highly different in  $\text{CrTe}_2/\text{In}_2\text{Te}_3(\uparrow)$  and  $\text{CrTe}_2/\text{In}_2\text{Te}_3(\downarrow)$ . By projecting the DOS onto  $\text{CrTe}_2$  and  $\text{In}_2\text{Te}_3$ , Fig. 2f shows that the projected DOS (PDOS) of  $\text{CrTe}_2$  in  $\text{CrTe}_2/\text{In}_2\text{Te}_3(\uparrow)$  is larger than that in  $\text{CrTe}_2/\text{In}_2\text{Te}_3(\downarrow)$  at Fermi level. Interestingly, the PDOS of  $\text{In}_2\text{Te}_3$  in  $\text{CrTe}_2/\text{In}_2\text{Te}_3(\uparrow)$  is larger than that in  $\text{CrTe}_2/\text{In}_2\text{Te}_3(\downarrow)$  below Fermi level while the situation is inversed above Fermi level (Fig. 2g). By looking into the five Cr-*d* orbital projected DOS in  $\text{CrTe}_2/\text{In}_2\text{Te}_3(\uparrow)$  and  $\text{CrTe}_2/\text{In}_2\text{Te}_3(\downarrow)$  (Fig. S5), we see that there are obviously different occupations for  $d_{xy}$ ,  $d_{x^2-y^2}$  and  $d_{3z^2-r^2}$  orbitals near Fermi level. All of these imply that the reversal of the FE polarization of  $\text{In}_2\text{Te}_3$  may have an unignorable influence on the magnetic properties of  $\text{CrTe}_2/\text{In}_2\text{Te}_3$ .

Due to the presence of the FE  $\text{In}_2\text{Te}_3$ , the inversion symmetry is inevitably broken and nonzero Dzyaloshinskii-Moriya interactions (DMIs) may exist in  $\text{CrTe}_2/\text{In}_2\text{Te}_3$ . In this case, we add a DMI term into Eq. (1) to investigate the magnetism of  $\text{CrTe}_2/\text{In}_2\text{Te}_3$  and the corresponding spin Hamiltonian is in the form of<sup>32</sup>

$$H = J_1 \sum_{\langle ij \rangle} S_i \cdot S_j + J_2 \sum_{\langle\langle ij \rangle\rangle} S_i \cdot S_j + \sum_{\langle ij \rangle} \mathbf{D}_{ij} \cdot (S_i \times S_j) - A \sum_i (S_i^z)^2 \quad (2).$$

In Eq. (2),  $\mathbf{D}_{ij}$  is the DMI vector of the NN Cr-Cr pairs. As the  $C_6$ -rotational symmetry with respect to Cr atoms in  $\text{CrTe}_2$  is reduced to the  $C_3$ -rotational symmetry, the NN DMIs are split into four different DMIs (Fig. S6). For simplicity, the  $J_1$  and  $J_2$  are still regarded to be six-fold. From Table I, we see that the NN  $J_1$  of both  $\text{CrTe}_2/\text{In}_2\text{Te}_3(\uparrow)$  and  $\text{CrTe}_2/\text{In}_2\text{Te}_3(\downarrow)$  are still FM but slightly smaller than that of free-standing  $\text{CrTe}_2$  ML. Moreover, the second-NN FM  $J_2$  is obviously enhanced in  $\text{CrTe}_2/\text{In}_2\text{Te}_3(\uparrow)$  compared with  $\text{CrTe}_2/\text{In}_2\text{Te}_3(\downarrow)$  and free-standing  $\text{CrTe}_2$  ML. To calculate the NN DMIs, we build a  $\sqrt{3} \times \sqrt{3}$  supercell of  $\text{CrTe}_2/\text{In}_2\text{Te}_3$  and the four-state method<sup>33</sup> is employed here. As

listed in Table S1, the FE polarization direction of  $\text{In}_2\text{Te}_3$  basically has no qualitative effect on the DMIs in  $\text{CrTe}_2/\text{In}_2\text{Te}_3$  although it affects their magnitudes. More explicitly, the magnitudes of the calculated DMIs range from 1.22 to 2.81 meV, which are about one order smaller than the NN  $J_1$ . Finally, we find that the SIA of  $\text{CrTe}_2/\text{In}_2\text{Te}_3$  is strongly dependent on the FE polarization of  $\text{In}_2\text{Te}_3$ . When  $\text{In}_2\text{Te}_3$  has an upward FE polarization, the SIA of  $\text{CrTe}_2/\text{In}_2\text{Te}_3(\uparrow)$  is negative, indicating an in-plane magnetic easy axis. However, when the FE polarization of  $\text{In}_2\text{Te}_3$  is downward,  $\text{CrTe}_2/\text{In}_2\text{Te}_3(\downarrow)$  has a positive SIA, indicating an out-of-plane magnetic easy axis. It is worth noting that  $\text{CrTe}_2/\text{In}_2\text{Te}_3(\downarrow)$  has a much weak SIA than the free-standing  $\text{CrTe}_2$  ML, although they both have positive SIAs. The different Heisenberg exchange couplings, DMIs and SIAs in  $\text{CrTe}_2/\text{In}_2\text{Te}_3(\uparrow)$  and  $\text{CrTe}_2/\text{In}_2\text{Te}_3(\downarrow)$  clearly unveil that the magnetic properties of  $\text{CrTe}_2$  are tuned by the FE polarization of  $\text{In}_2\text{Te}_3$ .

To obtain the magnetic ground state of  $\text{CrTe}_2/\text{In}_2\text{Te}_3$ , MC simulations are carried out. As shown in Fig. S7,  $\text{CrTe}_2/\text{In}_2\text{Te}_3(\uparrow)$  has an in-plane FM magnetic ground state whereas  $\text{CrTe}_2/\text{In}_2\text{Te}_3(\downarrow)$  has an out-of-plane one. Such magnetic ground states are understandable. Firstly, the ratios between DMIs and the NN Heisenberg exchange couplings are small and most of them are out of the typical range of 0.1–0.2 for the appearance of magnetic skyrmions.<sup>34</sup> Secondly, the SIAs of the  $\text{CrTe}_2/\text{In}_2\text{Te}_3(\uparrow)$  and the  $\text{CrTe}_2/\text{In}_2\text{Te}_3(\downarrow)$  prefer in-plane and out-of-plane magnetic easy axes, respectively. Taking them together, we obtain that the FM Heisenberg exchange couplings dominate over the DMIs and thus give rise to a FM magnetic ground state with its magnetization determined by the SIA,<sup>35</sup> consistent with our MC simulated results.

Figure 3a shows the  $\Gamma$ -dependent Gilbert dampings of  $\text{CrTe}_2/\text{In}_2\text{Te}_3$  with upward and downward FE polarizations of  $\text{In}_2\text{Te}_3$ . Similar to previous studies,<sup>36,37</sup> the Gilbert dampings of  $\text{CrTe}_2/\text{In}_2\text{Te}_3$  decrease first and then increase as the scattering rate  $\Gamma$  increases. Astonishingly, the Gilbert dampings of  $\text{CrTe}_2/\text{In}_2\text{Te}_3(\uparrow)$  and  $\text{CrTe}_2/\text{In}_2\text{Te}_3(\downarrow)$  are distinctly different at the same scattering rate  $\Gamma$  ranging from 0.001 to 1.0 eV. To have a more intuitive sense on the effect of the FE polarizations of  $\text{In}_2\text{Te}_3$  on the Gilbert dampings in  $\text{CrTe}_2/\text{In}_2\text{Te}_3$ , we calculate the ratio  $\eta = \alpha_\uparrow / \alpha_\downarrow$  at any given  $\Gamma$ , where

This is the author's peer reviewed, accepted manuscript. However, the online version of record will be different from this version once it has been copyedited and typeset.

PLEASE CITE THIS ARTICLE AS DOI: 10.1063/5.0145401

$\alpha_{\uparrow}(\alpha_{\downarrow})$  is the Gilbert damping of  $\text{CrTe}_2/\text{In}_2\text{Te}_3(\uparrow)$  [ $\text{CrTe}_2/\text{In}_2\text{Te}_3(\downarrow)$ ]. As shown in Fig. 3b, the ratio  $\eta$  ranges from 6 to around 1.3 with increasing  $\Gamma$ . As the FE polarization of  $\text{In}_2\text{Te}_3$  can be switched from upward to downward by an external electric field, the Gilbert damping of  $\text{CrTe}_2/\text{In}_2\text{Te}_3$  is electrically tunable in practice.

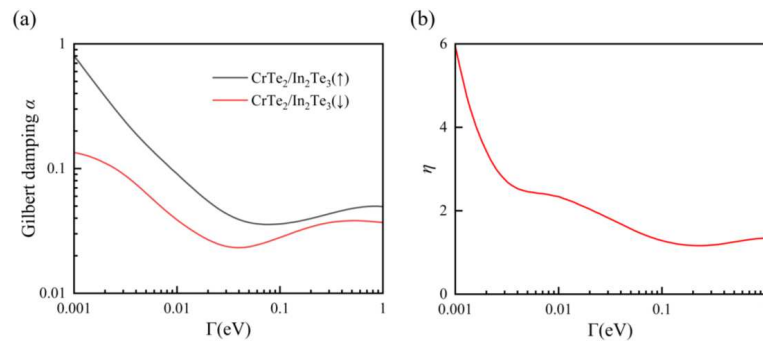


FIG. 3. (a) The  $\Gamma$ -dependent Gilbert dampings of  $\text{CrTe}_2/\text{In}_2\text{Te}_3$  with upward (black line) and downward (red line) FE polarizations of  $\text{In}_2\text{Te}_3$ . (b) The Gilbert damping ratio  $\eta$  as a function of the scattering rate  $\Gamma$ .

To gain a deep insight into how the FE polarization of  $\text{In}_2\text{Te}_3$  tunes the Gilbert damping in  $\text{CrTe}_2/\text{In}_2\text{Te}_3$ , we investigate the  $k$ -dependent contributions to the Gilbert dampings of  $\text{CrTe}_2/\text{In}_2\text{Te}_3(\uparrow)$  and  $\text{CrTe}_2/\text{In}_2\text{Te}_3(\downarrow)$ . As shown in Fig. 4a and 4b, the bands around Fermi level have quite different intermixing between  $\text{CrTe}_2$  and  $\text{In}_2\text{Te}_3$  states when the FE polarization of  $\text{In}_2\text{Te}_3$  is reversed. Explicitly, there are obvious intermixing below Fermi level in  $\text{CrTe}_2/\text{In}_2\text{Te}_3(\uparrow)$  while the intermixing mainly takes place above Fermi level in  $\text{CrTe}_2/\text{In}_2\text{Te}_3(\downarrow)$ . Especially, the bands intersected by Fermi level are at different  $k$  points in  $\text{CrTe}_2/\text{In}_2\text{Te}_3(\uparrow)$  and  $\text{CrTe}_2/\text{In}_2\text{Te}_3(\downarrow)$ . Through looking into the  $k$ -dependent contributions to their Gilbert dampings (Fig. 4c and 4d), we see that large contributions are from the  $k$  points (highlighted by arrows in Fig. 4) at which the bands of  $\text{CrTe}_2$  cross Fermi level. In addition, these large contributions are different. Such  $k$ -dependent contribution to Gilbert dampings is understandable. Based on the scattering

theory of Gilbert damping<sup>38</sup>, Gilbert damping parameter is calculated using the following Eq. (3)<sup>36</sup>

$$\alpha_{\mu\nu} = -\frac{\pi\hbar\gamma}{M_S} \sum_k \sum_{ij} \langle \psi_{k,i} | \frac{\partial \mathbf{H}_k}{\partial u_\mu} | \psi_{k,j} \rangle \langle \psi_{k,j} | \frac{\partial \mathbf{H}_k}{\partial u_\nu} | \psi_{k,i} \rangle \delta(E_F - E_{k,i}) \delta(E_F - E_{k,j}) \quad (3),$$

where  $E_F$  is Fermi level and  $E_{k,i}$  is the energy of band  $i$  at a given  $k$  point. Due to the delta  $\delta(E_F - E_{k,i})\delta(E_F - E_{k,j})$ , only the valence and conduction bands near Fermi level make dominant contribution to the Gilbert damping. Additionally, their contributions also depend on factor  $\langle \psi_{k,i} | \frac{\partial \mathbf{H}_k}{\partial u_\mu} | \psi_{k,j} \rangle \langle \psi_{k,j} | \frac{\partial \mathbf{H}_k}{\partial u_\nu} | \psi_{k,i} \rangle$ . Overall, through changing the intersections between the bands of CrTe<sub>2</sub> and Fermi level, the reversal of the FE polarization of In<sub>2</sub>Te<sub>3</sub> can modulate the contributions to Gilbert damping. Consequently, the total Gilbert dampings are different in CrTe<sub>2</sub>/In<sub>2</sub>Te<sub>3</sub>(↑) and CrTe<sub>2</sub>/In<sub>2</sub>Te<sub>3</sub>(↓).

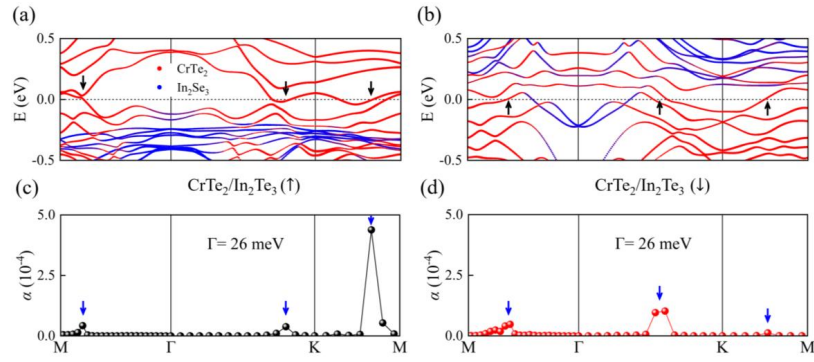


FIG. 4. (a) Band structure calculated with spin-orbit coupling and (c) the  $k$ -dependent contributions to the Gilbert damping in CrTe<sub>2</sub>/In<sub>2</sub>Te<sub>3</sub>(↑). (b) and (d) same as (a) and (c) but for CrTe<sub>2</sub>/In<sub>2</sub>Te<sub>3</sub>(↓). In (a) and (b), Fermi levels are indicated by horizontal dash lines and the states from CrTe<sub>2</sub> and In<sub>2</sub>Te<sub>3</sub> are shown by red and blue, respectively.

From experimental perspectives, the fabrication of CrTe<sub>2</sub>/In<sub>2</sub>Te<sub>3</sub> vdW heterostructure should be feasible. On the one hand, CrTe<sub>2</sub> with the lattice constant of

This is the author's peer reviewed, accepted manuscript. However, the online version of record will be different from this version once it has been copyedited and typeset.

PLEASE CITE THIS ARTICLE AS DOI: 10.1063/5.0145401

3.95 Å has been successfully grown on ZrTe<sub>2</sub> substrate by the molecular beam epitaxy.<sup>29</sup> On the other hand, In<sub>2</sub>Te<sub>3</sub> is also synthesized.<sup>39</sup> Taking these and the vdW nature of CrTe<sub>2</sub> and In<sub>2</sub>Te<sub>3</sub> together, a practical scheme of growing CrTe<sub>2</sub>/In<sub>2</sub>Te<sub>3</sub> is sketched in Fig. S8: first grow CrTe<sub>2</sub> ML on ZrTe<sub>2</sub> substrate<sup>29</sup> and then put In<sub>2</sub>Te<sub>3</sub> ML on CrTe<sub>2</sub> to form the desired CrTe<sub>2</sub>/In<sub>2</sub>Te<sub>3</sub> vdW heterostructure.

In summary, by constructing a vdW heterostructure of 2D FM metal CrTe<sub>2</sub> and FE In<sub>2</sub>Te<sub>3</sub> MLs, we find that the magnetic properties of CrTe<sub>2</sub> are engineered by the reversal of the FE polariton of In<sub>2</sub>Te<sub>3</sub>. Although the ferromagnetism of CrTe<sub>2</sub> is maintained in the presence of the FE In<sub>2</sub>Te<sub>3</sub>, its magnetic easy axis can be tuned from in-plane to out-of-plane by reversing the FE polarization of In<sub>2</sub>Te<sub>3</sub>. More importantly, the Gilbert damping of CrTe<sub>2</sub> is tunable with a wide range when reversing the FE polarization of In<sub>2</sub>Te<sub>3</sub> from upward to downward. Such tunability of the Gilbert damping in CrTe<sub>2</sub>/In<sub>2</sub>Te<sub>3</sub> results from the changed intersections between the bands of CrTe<sub>2</sub> and Fermi level on reversing the FE polarizations of In<sub>2</sub>Te<sub>3</sub>. Our work introduces a remarkably useful method to electrically tune the Gilbert dampings of 2D vdW FM metals by contacting them with ferroelectrics, and should stimulate more experimental investigations in this realm.

See the supplementary material for the details of computational methods<sup>31,36,40-50</sup> and other results mentioned in the main text.

This project is supported by National Nature Science Foundation of China (No. 12104518, 92165204, 11974432), NKRDPC-2018YFA0306001, NKRDPC-2022YFA1402802, GBABRF-2022A1515012643 and GZABRF-202201011118. Density functional theory calculations are performed at Tianhe-II.

#### AUTHOR DECLARATIONS

##### Conflict of Interest

The authors have no conflicts to disclose.

This is the author's peer reviewed, accepted manuscript. However, the online version of record will be different from this version once it has been copyedited and typeset.

PLEASE CITE THIS ARTICLE AS DOI: 10.1063/5.0145401

#### Author Contributions

**Liang Qiu:** Investigation (equal); Methodology (equal); Writing –original draft (equal).  
**Zequan Wang:** Methodology (equal). **Xiao-sheng Ni:** Investigation (equal); Methodology (equal). **Dao-Xin Yao:** Supervision (equal); Funding acquisition (equal); Investigation (equal); Writing – review & editing (equal). **Yusheng Hou:** Conceptualization (equal); Funding acquisition (equal); Investigation (equal); Project administration (equal); Resources (equal); Supervision (equal); Writing – review & editing (equal).

#### DATA AVAILABILITY

The data that support the findings of this study are available from the corresponding authors upon reasonable request.

#### REFERENCES

- <sup>1</sup> B. Huang, G. Clark, E. Navarro-Moratalla, D. R. Klein, R. Cheng, K. L. Seyler, D. Zhong, E. Schmidgall, M. A. McGuire, and D. H. Cobden, *Nature* **546**, 270 (2017).
- <sup>2</sup> C. Gong, L. Li, Z. Li, H. Ji, A. Stern, Y. Xia, T. Cao, W. Bao, C. Wang, Y. Wang, Z. Q. Qiu, R. J. Cava, S. G. Louie, J. Xia, and X. Zhang, *Nature* **546**, 265 (2017).
- <sup>3</sup> K. S. Burch, D. Mandrus, and J.-G. Park, *Nature* **563**, 47 (2018).
- <sup>4</sup> C. Gong and X. Zhang, *Science* **363**, eaav4450 (2019).
- <sup>5</sup> Q. H. Wang, A. Bedoya-Pinto, M. Blei, A. H. Dismukes, A. Hamo, S. Jenkins, M. Koperski, Y. Liu, Q.-C. Sun, and E. J. Telford, *ACS nano* **16**, 6960 (2022).
- <sup>6</sup> Y. Deng, Y. Yu, Y. Song, J. Zhang, N. Z. Wang, Z. Sun, Y. Yi, Y. Z. Wu, S. Wu, J. Zhu, J. Wang, X. H. Chen, and Y. Zhang, *Nature* **563**, 94 (2018).
- <sup>7</sup> A. F. May, D. Ovchinnikov, Q. Zheng, R. Hermann, S. Calder, B. Huang, Z. Fei, Y. Liu, X. Xu, and M. A. McGuire, *ACS nano* **13**, 4436 (2019).
- <sup>8</sup> M. Bonilla, S. Kolekar, Y. Ma, H. C. Diaz, V. Kalappattil, R. Das, T. Eggers, H.

This is the author's peer reviewed, accepted manuscript. However, the online version of record will be different from this version once it has been copyedited and typeset.

PLEASE CITE THIS ARTICLE AS DOI: 10.1063/5.0145401

- R. Gutierrez, M.-H. Phan, and M. Batzill, *Nature nanotechnology* **13**, 289 (2018).
- <sup>9</sup> W. Yu, J. Li, T. S. Heng, Z. Wang, X. Zhao, X. Chi, W. Fu, I. Abdelwahab, J. Zhou, and J. Dan, *Advanced Materials* **31**, 1903779 (2019).
- <sup>10</sup> D. J. O'Hara, T. Zhu, A. H. Trout, A. S. Ahmed, Y. K. Luo, C. H. Lee, M. R. Brenner, S. Rajan, J. A. Gupta, and D. W. McComb, *Nano letters* **18**, 3125 (2018).
- <sup>11</sup> B. Huang, M. A. McGuire, A. F. May, D. Xiao, P. Jarillo-Herrero, and X. Xu, *Nature Materials* **19**, 1276 (2020).
- <sup>12</sup> D. Zhong, K. L. Seyler, X. Linpeng, R. Cheng, N. Sivadas, B. Huang, E. Schmidgall, T. Taniguchi, K. Watanabe, M. A. McGuire, W. Yao, D. Xiao, K. C. Fu, and X. Xu, *Science advances* **3**, e1603113 (2017).
- <sup>13</sup> Y. Hou, J. Kim, and R. Wu, *Science Advances* **5**, eaaw1874 (2019).
- <sup>14</sup> C. Cardoso, D. Soriano, N. García-Martínez, and J. Fernández-Rossier, *Physical review letters* **121**, 067701 (2018).
- <sup>15</sup> B. Huang, G. Clark, D. R. Klein, D. MacNeill, E. Navarro-Moratalla, K. L. Seyler, N. Wilson, M. A. McGuire, D. H. Cobden, and D. Xiao, *Nature nanotechnology* **13**, 544 (2018).
- <sup>16</sup> Y. Xu, A. Ray, Y.-T. Shao, S. Jiang, K. Lee, D. Weber, J. E. Goldberger, K. Watanabe, T. Taniguchi, and D. A. Muller, *Nature Nanotechnology* **17**, 143 (2022).
- <sup>17</sup> X. Zhang, Q. Lu, W. Liu, W. Niu, J. Sun, J. Cook, M. Vaninger, P. F. Miceli, D. J. Singh, and S.-W. Lian, *Nature communications* **12**, 1 (2021).
- <sup>18</sup> X. Sun, W. Li, X. Wang, Q. Sui, T. Zhang, Z. Wang, L. Liu, D. Li, S. Feng, and S. Zhong, *Nano Research* **13**, 3358 (2020).
- <sup>19</sup> C. Ataca, H. Sahin, and S. Ciraci, *The Journal of Physical Chemistry C* **116**, 8983 (2012).
- <sup>20</sup> D. C. Freitas, R. Weht, A. Sulpice, G. Remenyi, P. Strobel, F. Gay, J. Marcus, and M. Núñez-Regueiro, *Journal of Physics: Condensed Matter* **27**, 176002

This is the author's peer reviewed, accepted manuscript. However, the online version of record will be different from this version once it has been copyedited and typeset.

PLEASE CITE THIS ARTICLE AS DOI: 10.1063/5.0145401

- (2015).
- 21 L. Meng, Z. Zhou, M. Xu, S. Yang, K. Si, L. Liu, X. Wang, H. Jiang, B. Li, and  
P. Qin, *Nature communications* **12**, 1 (2021).
- 22 P. Gao, X. Li, and J. Yang, *The Journal of Physical Chemistry Letters* **12**, 6847  
(2021).
- 23 J.-J. Xian, C. Wang, J.-H. Nie, R. Li, M. Han, J. Lin, W.-H. Zhang, Z.-Y. Liu,  
Z.-M. Zhang, and M.-P. Miao, *Nature communications* **13**, 1 (2022).
- 24 H. Lv, W. Lu, D. Shao, Y. Liu, and Y. Sun, *Physical Review B* **92**, 214419 (2015).
- 25 W. Eerenstein, M. Wiora, J. Prieto, J. Scott, and N. Mathur, *Nature materials* **6**,  
348 (2007).
- 26 S. Zhang, Y. Zhao, P. Li, J. Yang, S. Rizwan, J. Zhang, J. Seidel, T. Qu, Y. Yang,  
and Z. Luo, *Physical review letters* **108**, 137203 (2012).
- 27 H.-X. Cheng, J. Zhou, C. Wang, W. Ji, and Y.-N. Zhang, *Physical Review B* **104**,  
064443 (2021).
- 28 S. Manzeli, D. Ovchinnikov, D. Pasquier, O. V. Yazyev, and A. Kis, *Nature*  
*Reviews Materials* **2**, 1 (2017).
- 29 Y. Ou, W. Yanez, R. Xiao, M. Stanley, S. Ghosh, B. Zheng, W. Jiang, Y.-S.  
Huang, T. Pillsbury, and A. Richardella, *Nature communications* **13**, 1 (2022).
- 30 C. Xu, J. Feng, H. Xiang, and L. Bellaiche, *npj Computational Materials* **4**, 1  
(2018).
- 31 S. Li, S.-S. Wang, B. Tai, W. Wu, B. Xiang, X.-L. Sheng, and S. A. Yang,  
*Physical Review B* **103**, 045114 (2021).
- 32 X.-S. Ni, C.-Q. Chen, D.-X. Yao, and Y. Hou, *Physical Review B* **105**, 134406  
(2022).
- 33 H. Xiang, E. Kan, S.-H. Wei, M.-H. Whangbo, and X. Gong, *Physical Review*  
*B* **84**, 224429 (2011).
- 34 A. Fert, V. Cros, and J. Sampaio, *Nature Nanotechnology* **8**, 152 (2013).
- 35 S. Banerjee, J. Rowland, O. Erten, and M. Randeria, *Physical Review X* **4**,  
031045 (2014).

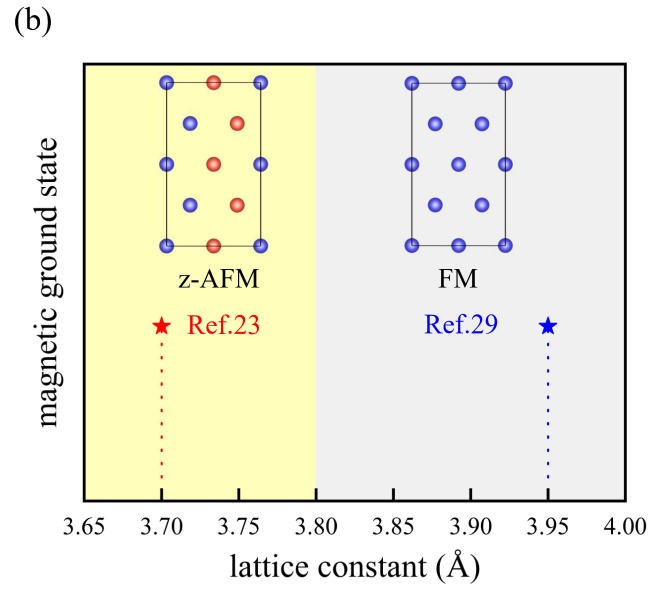
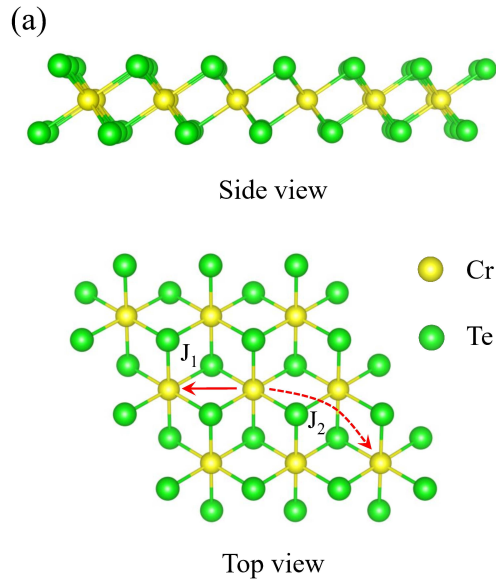
This is the author's peer reviewed, accepted manuscript. However, the online version of record will be different from this version once it has been copyedited and typeset.

PLEASE CITE THIS ARTICLE AS DOI: 10.1063/5.0145401

- 36 Y. Hou and R. Wu, *Physical Review Applied* **11**, 054032 (2019).
- 37 K. Gilmore, Y. Idzerda, and M. D. Stiles, *Physical review letters* **99**, 027204  
(2007).
- 38 A. Brataas, Y. Tserkovnyak, and G. E. W. Bauer, *Physical Review Letters* **101**,  
037207 (2008).
- 39 B. Chen, F. Fei, D. Zhang, B. Zhang, W. Liu, S. Zhang, P. Wang, B. Wei, Y.  
Zhang, Z. Zuo, J. Guo, Q. Liu, Z. Wang, X. Wu, J. Zong, X. Xie, W. Chen, Z.  
Sun, S. Wang, Y. Zhang, M. Zhang, X. Wang, F. Song, H. Zhang, D. Shen, and  
B. Wang, *Nature Communications* **10**, 4469 (2019).
- 40 G. Kresse and J. Hafner, *Physical review B* **47**, 558 (1993).
- 41 G. Kresse and J. Furthmüller, *Physical review B* **54**, 11169 (1996).
- 42 P. E. Blöchl, *Physical review B* **50**, 17953 (1994).
- 43 G. Kresse and D. Joubert, *Physical review b* **59**, 1758 (1999).
- 44 H. J. Monkhorst and J. D. Pack, *Physical review B* **13**, 5188 (1976).
- 45 V. Wang, N. Xu, J.-C. Liu, G. Tang, and W.-T. Geng, *Computer Physics  
Communications* **267**, 108033 (2021).
- 46 S. L. Dudarev, G. A. Botton, S. Y. Savrasov, C. Humphreys, and A. P. Sutton,  
*Physical Review B* **57**, 1505 (1998).
- 47 X. Sui, T. Hu, J. Wang, B.-L. Gu, W. Duan, and M.-s. Miao, *Physical Review B*  
**96**, 041410 (2017).
- 48 S. Grimme, J. Antony, S. Ehrlich, and H. Krieg, *The Journal of chemical physics*  
**132**, 154104 (2010).
- 49 X. Wang, R. Wu, D.-s. Wang, and A. Freeman, *Physical Review B* **54**, 61 (1996).
- 50 J. Hu and R. Wu, *Physical Review Letters* **110**, 097202 (2013).

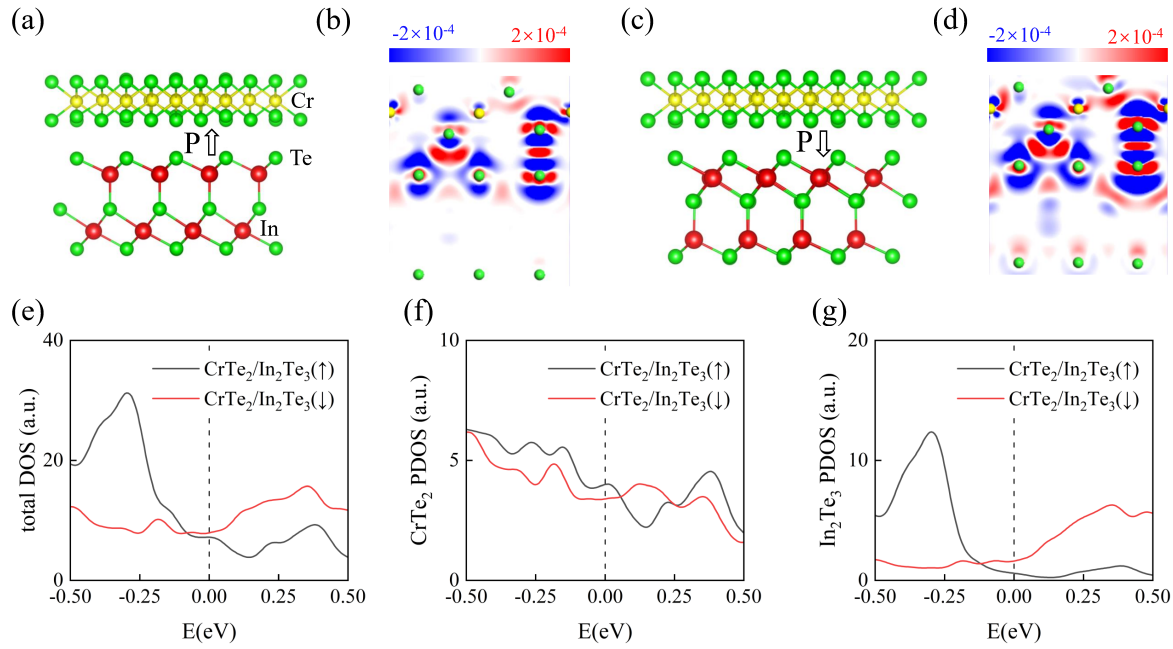
This is the author's peer reviewed, accepted manuscript. However, the online version of record will be different from this version once it has been copyedited and typeset.

PLEASE CITE THIS ARTICLE AS DOI: 10.1063/5.0145401



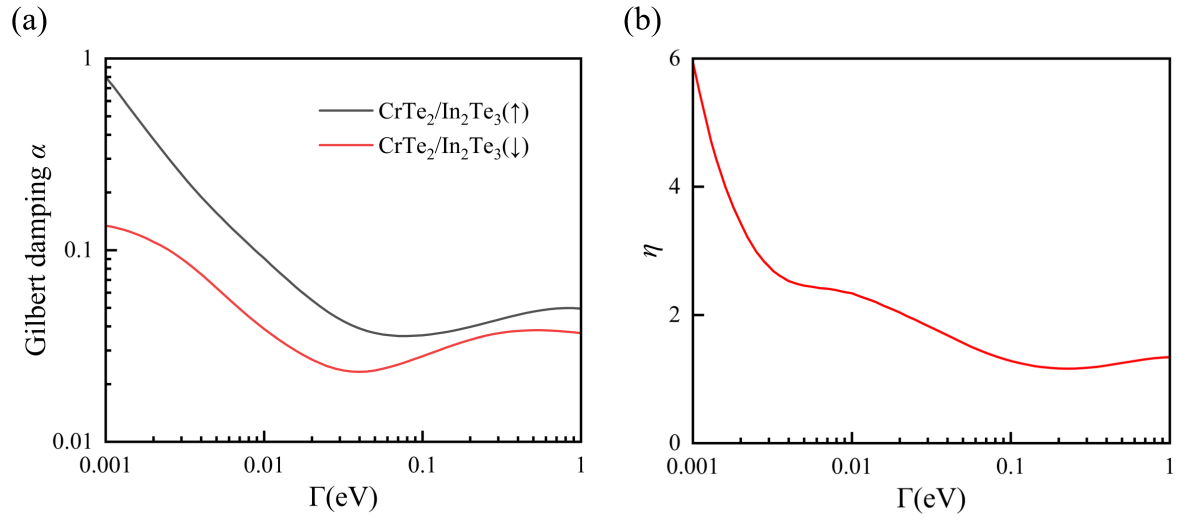
This is the author's peer reviewed, accepted manuscript. However, the online version of record will be different from this version once it has been copyedited and typeset.

PLEASE CITE THIS ARTICLE AS DOI: 10.1063/1.50145401



This is the author's peer reviewed, accepted manuscript. However, the online version of record will be different from this version once it has been copyedited and typeset.

PLEASE CITE THIS ARTICLE AS DOI: 10.1063/5.0145401



This is the author's peer reviewed, accepted manuscript. However, the online version of record will be different from this version once it has been copyedited and typeset.

PLEASE CITE THIS ARTICLE AS DOI: 10.1063/5.0145401

